International Journal of Mechanical Engineering and Technology (IJMET)
Volume 10, Issue 01, January 2019, pp. 1221-1234, Article ID: IJMET_10_01_124
Available online at http://www.iaeme.com/ijmet/issues.asp?JType=IJMET&VType=10&IType=1
ISSN Print: 0976-6340 and ISSN Online: 0976-6359

NUMERICAL INVESTIGATION OF SHELL-AND-TUBE HEAT EXCHANGER WITH PARABOLIC SEGMENTAL BAFFLE CUT

Ikpotokin I., Uguru-Okorie D. C. and Osueke C. O.
Department of Mechanical Engineering
Landmark University, Omu-Aran, Kwara State, Nigeria

A. A. Dare and M. O. Petinrin
Department of Mechanical Engineering
University of Ibadan, Oyo State, Nigeria

ABSTRACT

An investigation was carried out on the effect of the use of a parabolic baffle at different baffle cuts on the performance of shell and tube heat exchangers. The numerical study was performed on a personal computer with 12 GB RAM and Intel® Core™ i7 2.50GHz CPU using a CFD software Comsol Multiphysics. The modeled heat exchanger had 37 tubes, shell internal diameter of 200 mm, 6 baffles with baffle spacing of 100 mm. The results from the effect of mass flow rate and baffle cut on heat transfer rate and pressure drop in the shell side of the heat exchanger were compared with the circular segmental baffle cut of 25% and that of the parabolic baffle cut of 25 and 30% of the inner shell diameter. At 25% of the shell diameter baffle cut, the parabolic cut had an improved heat transfer rate compared to that with the circular segmental baffle cut with a drawback of higher pressure drop. As the parabolic baffle cuts increased, there was a decrease in heat transfer rates and pressure drops at the various mass flow rates considered. At 30% of shell diameter cut, the performance of the parabolic segmental baffle cut gave results similar to the circular segmental baffle cut at 25% of the inner shell diameter. The investigation showed that for a parabolic baffle cut, 30% of the shell diameter is recommended for optimum performance..

Keywords: Shell and tube heat exchanger, baffle cut, heat transfer, pressure drop, fluid flow.

Cite this Article: Ikpotokin I., Uguru-Okorie D. C. Osueke C. O., A. A. Dare and M. O. Petinrin, Numerical Investigation of Shell-and-Tube Heat Exchanger with Parabolic Segmental Baffle Cut, International Journal of Mechanical Engineering and Technology, 10(01), 2019, pp. 1221-1234-.
http://www.iaeme.com/IJMET/issues.asp?JType=IJMET&VType=10&IType=1

1. INTRODUCTION

Energy crunch, environmental pollution, climate change, global warming, instability in energy prices and excessive heat dissipation are very serious challenges all around the world. These situations have continued to generate interests in promoting and development of technologies to reduce energy consumption and improve conversion efficiency with a view of saving energy and mitigating environmental impact. One of the most efficient and reliable means used in thermal systems to achieve the above goals involves improving the thermal performance of heat exchangers via geometrical retrofitting of components particularly baffles in shell-and-tube exchanger units [1-3].

Heat exchangers are process devices used for the transfer of thermal energy primarily between two fluid streams at different temperatures. Different types of heat exchanger ranging from double pipe, coiled tube, shell-and-tube to extended surface to plate design exist [4]. Among them, the shell-and-tube heat exchangers are the commonly used ones in power and process industries because of their versatility, reliable operation at various operating conditions and environments, ease of maintenance and repair, possibility for upgrade and custom design [5].

Baffles are incorporated in the shell section to support the tube bundles and direct the shell side-flow relative to the tubes resulting in increase in turbulence and heat transfer coefficient, in the shell-and-tube heat exchanger type. In addition to structural support and improvement of heat transfer, baffles also increase pressure drop [6]. The earlier effects of baffles are considered to determine the number of baffles that may be used.

The shell-and-tube heat exchangers with segmental baffles are mostly employed in various industrial applications because of their ease of fabrication, installation, substantial heat transfer rate and low cost. However, these exchangers are experiencing relatively higher challenges in service performance due to inherent flow and heat transfer problems such as non-uniform mixing, acute flow instability, flow induced vibration, flow stagnation zones, high pressure drop, fouling and corrosion [7-8].

The above demerits have spurred interests to develop several configurations of new baffles ranging from orifice baffles, rod baffles, helical baffles, disc and doughnut baffles, to ladder-type baffles. However, these new baffles also have their own challenges in many applications. For instance, the development of orifice baffle was intended to reduce dead regions while the rod baffles were design to reduce flow instabilities coupled with the attendant effect of flow induced vibration. Since these baffles are associated with axial flow, the resulting heat transfer performance is low compared to that of segmental baffled shell-and-tube heat exchanger. In order to increase the shell side heat transfer, the exchangers usually become relatively large, thus increasing its cost production [9-13].

In the past three decades, the introduction of helical baffles has attracted a great deal of research interest because of the anticipated significant improvement in heat transfer rates, pressure drop and vibration reduction [14]. Nevertheless, a comparative study conducted by Chen et al [15] and Jian-Fei et al [16] revealed that shell-and-tube heat exchanger with plane segmental baffles has higher thermal performance and lower pressure drop than those with helical baffles. The inherent leakage zones in exchanger with non-continuous helical baffled specifically are inimical to the heat transfer rates [17]. In addition to the thermal drawback of helical baffled shell-and-tube heat exchanger, the cost of manufacturing and maintenance is very high compared to that of a conventional segmental baffled heat exchanger.

Due to the well-established standards for designing and manufacturing segmental baffled shell-and-tube heat exchanger coupled with the low cost of fabrication and wild spread use in many industries, several studies have been carried out related to the conventional baffles with

a view of optimizing the shell-side performance. A lot of research efforts were focused on the effect of baffle spacing, baffle orientation and use of multiple baffles [18-19]. In all the studies related to segmental baffles, the flow window is mainly of circular cut. There is no investigator to the best of the author's knowledge, who have used a parabolic segmental cut. Therefore, in this study the potential effect of a parabolic segmental cut on the shell side thermal performance of a shell-and-tube heat exchanger is investigated numerically.

This study involves the modeling and studying of parabolic segmental cut at different levels. A conventional shell-and-tube heat exchanger with circular segmental baffle cut was employed for comparison. The numerical study was performed on a personal computer with 12 GB RAM and Intel® Core™ i7 2.50GHz CPU using a Computational Fluid Dynamics (CFD) software Comsol Multiphysics.

2. COMPUTATIONAL MODELS

2.1. Geometric model

Table 1 Specifications of the computation domain

Parameter	Value
Number of tubes	37
Number of baffles	6
Outer diameter of tube (mm)	15
Tube length (mm)	620
Tube layout	Triangular
Shell internal diameter (mm)	200
Baffle spacing (mm)	100
Inlet/outlet nozzle diameter (mm)	50
Tube material	Copper
Shell/baffle material	Steel
Working fluid	Water

A three-dimensional (3D) model of the Shell-and-tube heat exchanger with parabolic segmental baffles on which the mathematical equations representing the flow field variables are to be solved is depicted in figure 1 and the specifications are given in Table 1.

The model has a single shell and tube passes. The model was created in Solidworks and introduced into the CAD module interface in COMSOL Multiphysics computational fluid dynamics software via the livelink.

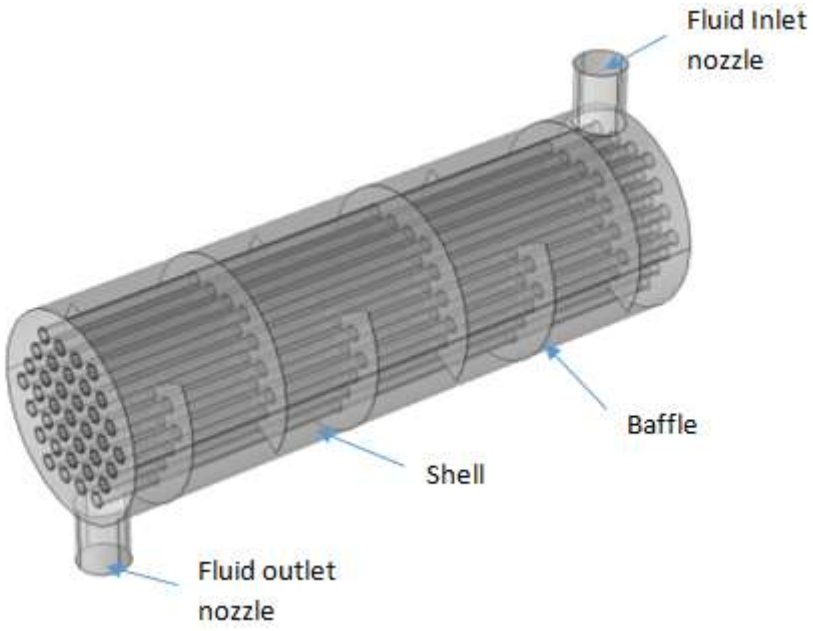

Figure 1 Computational domain

Detailed configuration of the circular and parabolic segmental cut baffles is presented in figure 2.

The parabolic segmental baffle is characterized by the focus (*f*) and vertex (*v*) as shown in figure 2 (b). The height, *h* of the parabola is the distance between the focus and vertex.

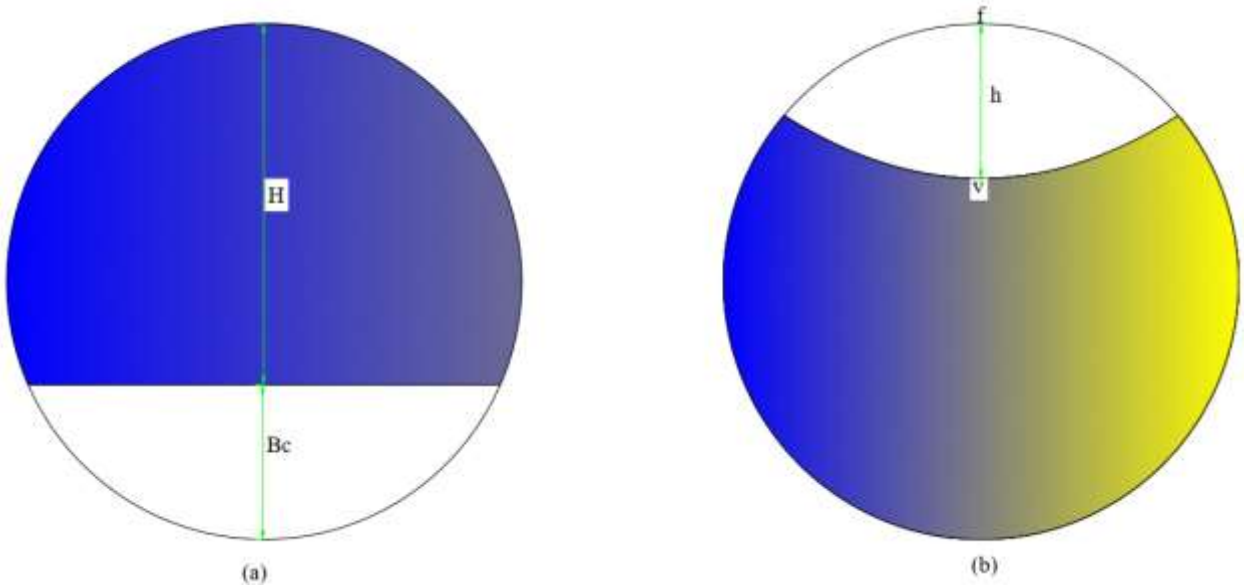

Figure 2 Baffles (a) Circular segmental cut and (b) Parabolic segmental baffle cut

Where *Bc* is baffle cut and *H* is baffle height.

Table 2 Material property

Property	**Numerical value**
Copper	
Density	8933 kg/m^3
Thermal conductivity	401 W/m.K
Specific heat capacity at constant pressure	385 J/kg.K
Steel	
Density	8055 kg/m^3
Thermal conductivity	15.1 W/m.K
Specific heat capacity at constant pressure	480 J/kg.K

The material properties of interest for copper and steel are depicted in table 2. Water was used in this study as the working fluid. The properties of the working fluid are dependent on the average temperature at inlet and outlet of the exchanger.

2.2. Governing equations or mathematical model

Numerical solution of heat transfer and fluid flow behavior involves solving conservation equations. In this investigation, the governing equations were formulated under the following assumptions:

i. The flow is incompressible.
ii. The flow is turbulent.
iii. Gravity effect, volume force, heat source and thermal radiation are negligible.
iv. The fluid is a single-phase Newtonian fluid.

Based on these assumptions, the governing conservation equations for continuity, momentum, energy, turbulent kinetic energy k and turbulent dissipation rate ε written in vector forms are solved. The equations are as follows:

Continuity equation:

$$\frac{\partial \rho}{\partial t} + \rho \boldsymbol{\nabla}.\boldsymbol{u} = 0 \tag{1}$$

Momentum equation:

$$\rho \frac{\partial \boldsymbol{u}}{\partial t} + \rho \boldsymbol{u}.\nabla \boldsymbol{u} = -\nabla p + \nabla.\left(\mu(\nabla \boldsymbol{u} + (\nabla \boldsymbol{u})^T) - \frac{2}{3}\mu(\nabla.\boldsymbol{u})\boldsymbol{I}\right) \tag{2}$$

Energy equation:

$$\rho C_p \left(\frac{\partial T}{\partial t} + \boldsymbol{u}.\nabla T\right) + \nabla q = -\frac{T}{\rho}\frac{\partial \rho}{\partial T}\left(\frac{\partial p}{\partial t} + \boldsymbol{u}.\nabla p\right) + \Phi \tag{3}$$

Turbulent kinetic energy equation:

$$\rho \frac{\partial k}{\partial t} + \rho \boldsymbol{u}.\nabla k = \nabla.\left(\left(\mu + \frac{\mu_T}{\sigma_k}\right)\nabla k\right) + \boldsymbol{P}_k - \rho\varepsilon \quad (4)$$

Turbulent energy dissipation rate equation:

$$\rho \frac{\partial \varepsilon}{\partial t} + \rho \boldsymbol{u}.\nabla \varepsilon = \left(\left(\mu + \frac{\mu_T}{\sigma_\varepsilon}\right)\nabla \varepsilon\right) + C_{\varepsilon 1}\frac{\varepsilon}{k}P_k - C_{\varepsilon 2}\rho\frac{\varepsilon^2}{k} \quad (5)$$

Where,

ρ = fluid density

$\boldsymbol{u}$ = velocity vector

$\boldsymbol{I}$ = unit vector

p = pressure

μ = dynamic viscosity

C_p= specific heat capacity at constant pressure

T = absolute temperature

q = heat flux by conduction

Φ = viscous dissipation function

$\boldsymbol{P}_k$ = production term = $\mu_T\left(\nabla \boldsymbol{u}: (\nabla \boldsymbol{u} + (\nabla \boldsymbol{u})^T - \frac{2}{3}(\nabla.\boldsymbol{u})^2\right) - \frac{2}{3}\rho k \nabla.\boldsymbol{u}$

μ_T = turbulent viscosity = $\rho C_\mu \frac{k^2}{\varepsilon}$

$C\mu$, $C_{\varepsilon 1}$, $C_{\varepsilon 2}$, σ_k *and* σ_ε are model constant with value 0.09, 1.44, 1.92 and 1.3 respectively.

2.3. Boundary conditions

The boundary conditions specified for the heat exchanger shown in figure 1 are as follows:

a) Inlet of the computational domain is set to uniform velocity and temperature as
   i. u = w = 0, v = uniform velocity.
   ii. T_{in} = uniform temperature (293 K).

b) Inlet turbulent intensity $I_T$and turbulent length scale L_T values are related to the turbulent variables via

$$k = \frac{3}{2}(|\mathbf{u}|I_T)^2 \text{ and } \varepsilon = C_\mu^{3/4}\frac{k^{3/2}}{L_T}$$

c) Outlet of the computational domain is set as

$$\frac{\partial u}{\partial n} = 0,\ \frac{\partial v}{\partial n} = 0,\ \frac{\partial w}{\partial n} = 0,\ \frac{\partial T}{\partial n} = 0,\ \frac{\partial k}{\partial n} = 0,\ \frac{\partial \varepsilon}{\partial n} = 0$$

d) Impermeable boundary and wall function conditions were implemented over the tube wall as well as the shell and baffle surfaces.

e) A constant temperature of tube wall is maintained at 352 K, while adiabatic wall conditions were assumed for the shell and baffles surfaces.

2.4. Mesh generation

Since the shell side of shell-and-tube heat exchanger has a complex flow geometry, unstructured tetrahedral elements were adopted for mesh generation as shown in figure 3. In order to obtain accurate numerical results, mesh independent tests were conducted. Four

different meshes were generated for the conventional baffled and parabolic baffled computational domains.

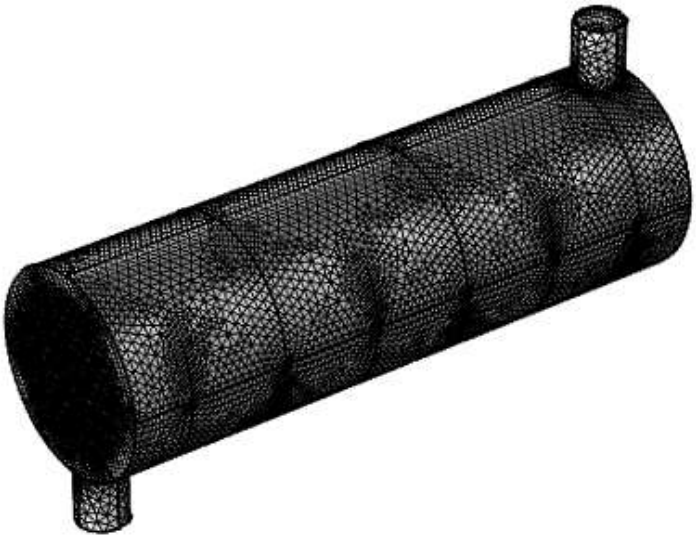

Figure 3 Computational mesh

3. NUMERICAL METHOD

The numerical simulations were performed using Comsol Multiphysics 5.3. The multigrid algorithm was employs to solve for the field flow variables. The convergence criterion for the relative residual was set to 10^{-5}. The processing time for each computation on personal computer with specifications 12 GB RAM Intel® Core™ i7 2.50GHz CPU was approximately 19 hours.

The mass flow rate was calculated from equation (1).

$$\dot{m} = \rho UA \tag{6}$$

The rate of heat transfer with the expression:

$$Q = \dot{m}C_p(\dot{T}_{out} - T_{in}) \tag{7}$$

The average convective heat transfer coefficient was expressed as:

$$h = \frac{Q}{A_s \Delta T_{ln}} \tag{8}$$

$$\Delta T_{ln} = \frac{(T_w - T_{in}) - (T_w - T_{out})}{\ln[(T_w - T_{in})/(T_w - T_{out})]} \tag{9}$$

$$A_s = N_t \pi d_o l \tag{10}$$

Where,

ρ is the working fluid's density, U is the inlet fluid flow velocity and A is exchanger inlet flow cross-sectional area, T_{out} and T_{in} are the outlet and inlet fluid temperatures respectively, C_p is the specific heat capacity of the fluid (water) at constant pressure, A_s is heat transfer surface area, N_t is number of tubes, d_o tube outer diameter, l is tube length, and ΔT_{ln} is logarithm mean temperature difference.

4. RESULT AND DISCUSSION

The numerical results of this study are divided into the three parts: mesh independent test, numerical validation and heat exchanger performance.

4.1. Mesh independent tests

The results obtained for four different meshes with a constant flow rate maintain at 2.35 kg/s, are presented in table 3. For the conventional baffle heat exchanger with circular segmental baffles, the heat transfer coefficient and drop pressure decrease by 0.59 and 1.2% respectively as the number of mesh increased from 1256693 to 1437076. Similarly, the heat transfer coefficient and pressure drop associated with parabolic segmental baffled heat exchanger decreased by 0.68 and 1.27% respectively as the mesh number increased from 1324649 to 1480770. Considering both computation time and solution accuracy, 1256693 and 1324649 mesh were adopted for circular and parabolic cut baffled exchanger respectively.

Table 3 Mesh independent test results

Mesh number		h ($W/m^2.K$)			Δp (Pa)	
Circular cut segmental baffled exchanger model						
668072		2059.9			3155.8	
972710		2622.2			3600.7	
1256693		2617.9			3593.8	
1437076		2602.5			3549.7	
Parabolic cut segmental baffled exchanger model						
681401		2216.7			4953.6	
959069		2225.3			4302.4	
1324649		2775.4			4758.1	
1480770		2756.7			4697.9	

4.2. Numerical solution validation

Since there are scarce literatures related to both empirical and numerical study of parabolic cut segmental baffled shell-and-tube heat exchangers, a conventional shell-and-tube heat exchanger with circular segmental baffle cut of 25% inner shell diameter was modeled and numerically investigated. The results were compared with those gotten using empirical correlation developed by Kern [20] as presented in figures 4 and 5. It can be seen from these figures showing the results, that both the rate of heat transfer and pressure drop obtained from the simulation and use of the empirical correlation by Kern method, showed increase with increase in mass flow rate. However, an average difference of 4.8 and 10.7% was observed from the results obtained numerically and with Kern method for heat transfer rate and

pressure drop respectively. Based on the preceding percentage error involved, this present numerical simulation provides satisfactory prediction of heat transfer and pressure drop.

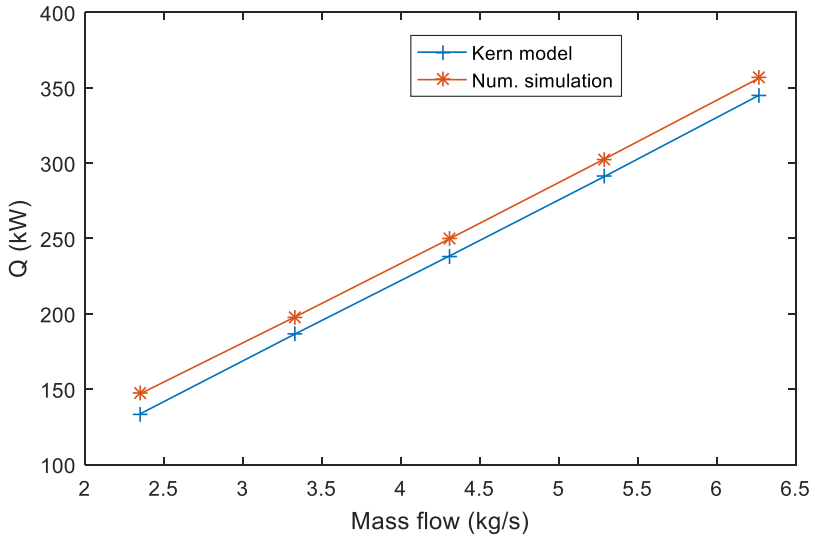

Figure 4 Rate of heat transfer using Kern model and numerical simulation

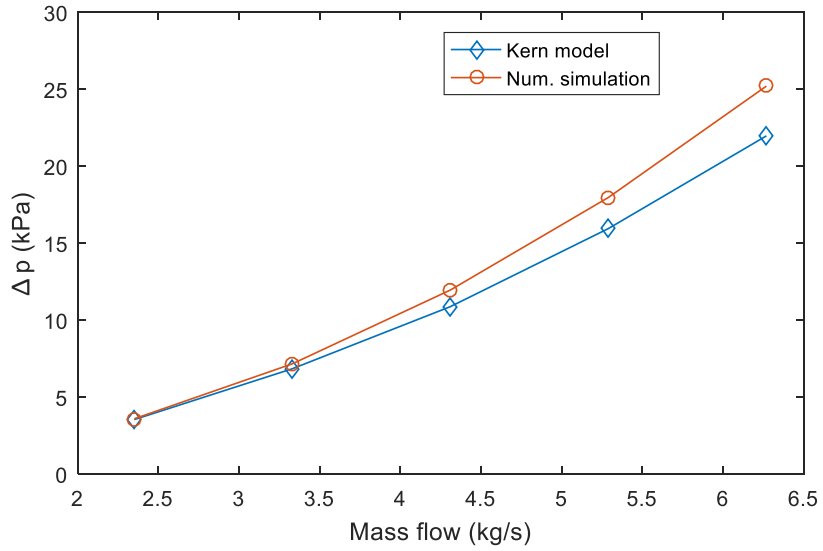

Figure 5 Pressure drop using Kern model and Numerical simulation

4.3. Effect of parabolic baffle cut on heat transfer coefficient

The heat transfer coefficient for 50, 60, 70, 80 and 90 mm parabolic baffle cut heights which represents 25, 30, 35, 40 and 45% respectively of the internal diameter of the shell side of the heat exchanger are presented in figure 6. For the five different baffle cut heights, heat transfer coefficient increased with the increase of mass flow rate. Parabolic baffle with cut height of 50 mm had higher heat transfer coefficient followed by that of 60, 70, 80 and lowest for 90 mm baffle cut. As the level of baffle cut increased, the heat transfer coefficient decreased indicating the reduction in turbulence and mixing of the shell-side fluid flow due to the greater cross flow windows.

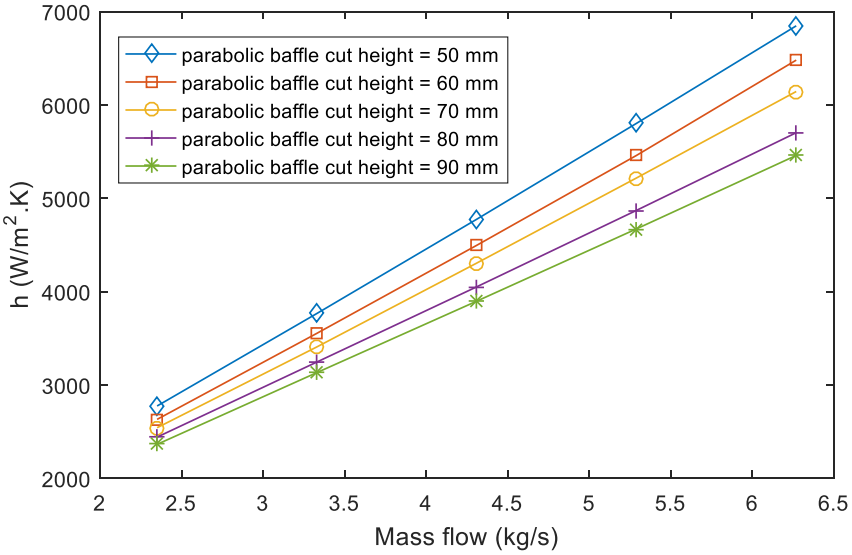

Figure 6 Heat transfer coefficient for baffle cut height vs. flow rate

4.4. Effect of parabolic baffle cut on heat duty

Improving the shell-side flow heat transfer coefficient of a shell-and-tube heat exchanger will have a corresponding effect on the heat duty or rate of heat transfer. The rate of heat transfer at five levels of flow rate for 50, 60, 70, 80 and 90 mm parabolic baffle cut height are presented in figure 7. The heat transfer rate increased as the level of parabolic baffle cut height decreased from 90 to 50 mm and the heat transfer rate was also observed to increase with increase in mass flowrate of the fluid. The highest rate of heat transfer was observed at the baffle cut height of 50 mm. The results show that the rate of heat transfer is dependent on both the flow rate and baffle cut height.

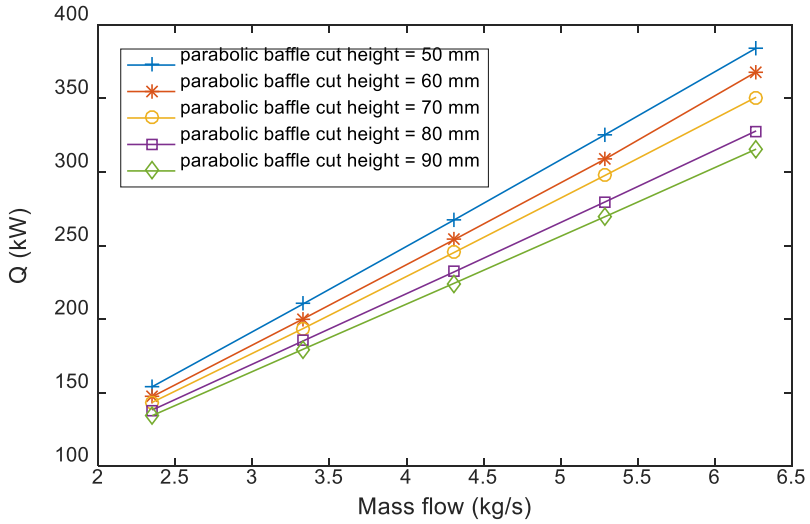

Figure 7 Heat duty for baffle cut height vs. flow rate

4.5. Effect of parabolic baffle cut on pressure drop

Pressure drop is one of the important paramters required to determine the pressure and power required to move fluid on the shell-side of a shell-and-tube heat exchanger. The effect of

parabolic baffle cut height on pressure drop for parabolic baffle cut heights of 50, 60, 70, 80 and 90 mm are presented in figure 8. It is observed that pressure drop increased as the parabolic baffle cut height reduced from 90 to 50 mm. This can be attributed to the larger flow cross section created by increasing the baffle cut and in addition, an indication of reduction in flow turbulence which is associated with flow induced vibration. A lower pressure drop reduces the pumping power in the exchanger.

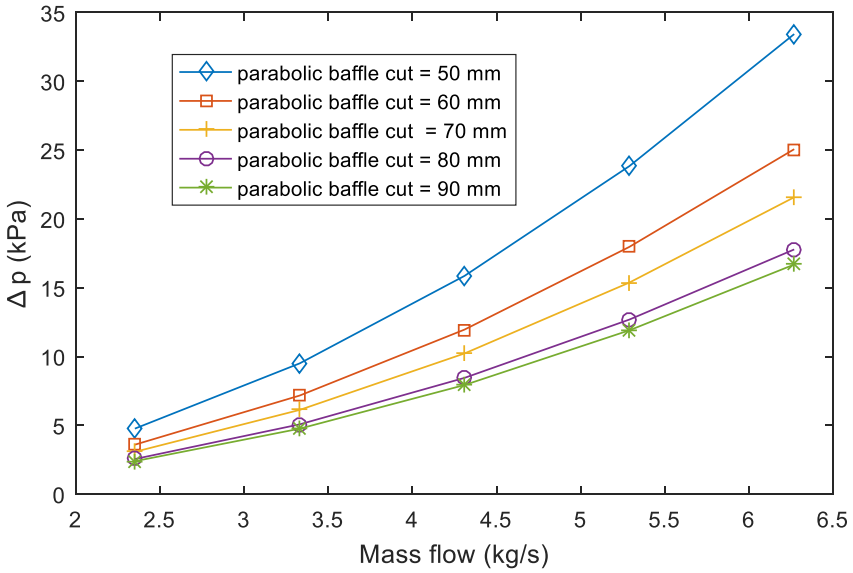

Figure 8 Pressure drop for parabolic baffle cut vs. flow rate

4.6. Comparing parabolic and circular segmental baffle cut

In order to ascertain how well parabolic segmental baffle cut performs on the shell-side of a shell-and-tube exchanger, results of selected baffle cut heights were compared with that of circular segmental baffle cut of 50 mm (i.e 25% inner shell diameter). The heat transfer rate and the pressure drop of 50 and 60 mm parabolic baffle cut heights were compared to circular segmental baffle cut of 50 mm as presented in figures 9 and 10. The heat transfer rates of the two different parabolic baffles cut heights of 50 and 60 mm were observed to be higher than the circular baffle cut for all the various flow rates tested. At 30% of shell diameter cut, the performance of the parabolic segmental baffle gave results similar to the circular segmental baffle cut at 25% of the shell diameter.

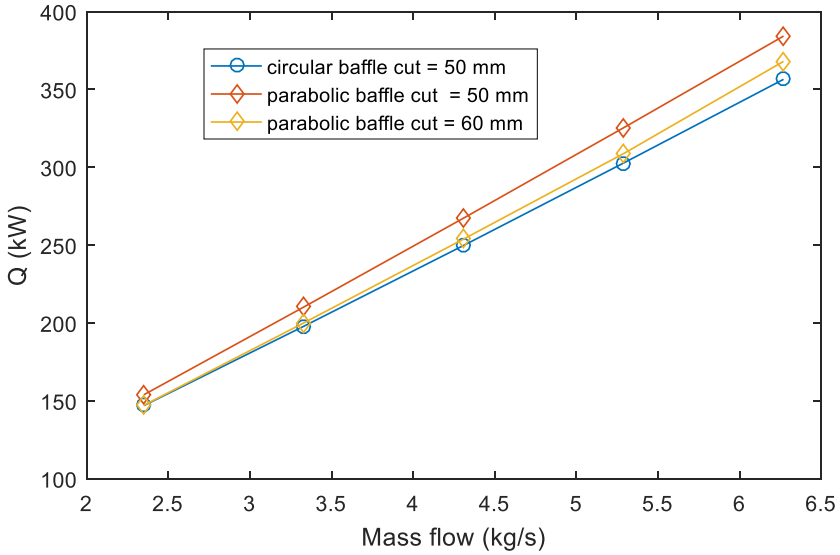

Figure 9. Comparing heat transfer rate for parabolic and circular segmental baffle cut

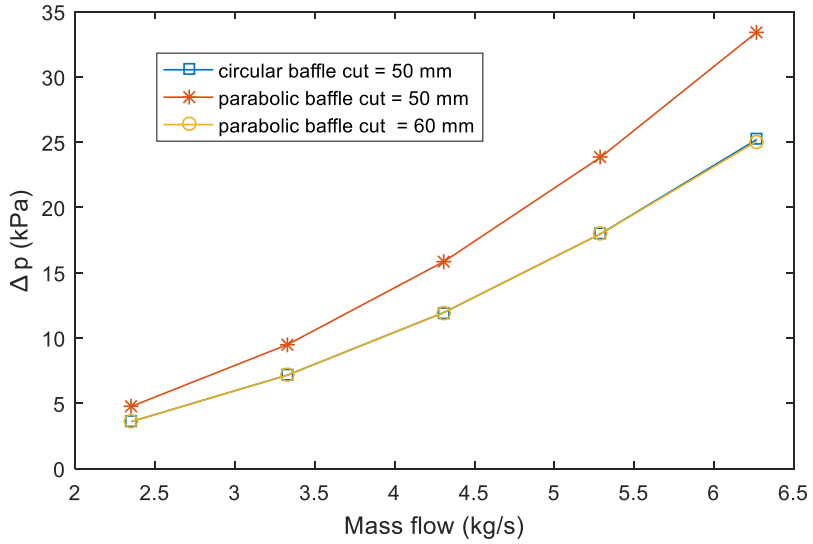

Figure 10. Comparing pressure drop for parabolic and circular segmental baffle cut

5. CONCLUSION

A heat exchanger with a segmental baffle cut of 25% of the shell diameter was modeled and the performance was compared with the performance of a parabolic segmental baffle cut of 25, 30, 35, 40 and 45% of the inner shell diameter. The following are the findings:-

i. The 25% of shell diameter baffle cut of the parabolic segmental baffle gave a better heat transfer rate when compared to the circular segmental baffle cut at 25% of shell diameter but had a higher pressure drop when compared to the circular segmental baffle.

ii. At 30% of inner shell diameter baffle cut, the performance of the parabolic segmental baffle gave results similar to the circular segmental baffle cut at 25% of the shell diameter.

iii. At 30, 35, 40 and 45% of inner shell diameter baffle cut, the heat transfer rate and pressure drop in the parabolic segmental baffle heat exchanger reduced with increase in baffle cut.

iv. For optimum performance, 25% of inner shell diameter baffle cut is recommended for the circular segmental baffle cut and 30% of the inner shell diameter for a parabolic baffle cut is recommended for optimum performance.

REFERENCES

[1] Quan C., Karen F., Hanning L., Xiaohui Z., Jue Z., Vida S., and Jim S. Condensing Boiler Applications in Process Industry. *Applied Energy*, **89**, 2012, pp. 30-35.

[2] Petr S. and Vishwas V. W. Different Strategies to Improve Industrial Heat Exchange. *Heat Transfer Engineering*, **23**(6), 2002, pp. 36-48.

[3] Xinting W., Nianben Z., Zhichun L., and Wei L. Numerical Analysis and Optimization Study on Shell-side Performances of a Shell and tube Heat Exchanger with Staggered Baffles. *International Journal of Heat and Mass Transfer*, **124**, 2018, pp. 247-259.

[4] Kuppan T. Heat Exchanger Design Handbook, 2nd Edition. New York:CRC Press, 2013, pp. 2-27.

[5] Master, B., Chunangad, K. S., Boxma, A. J., Kral, D., and Stehlik, P. Most Frequently used Heat Exchangers from Pioneering Research to Worldwide Applications. *Heat Transfer Engineering*, **27**(6), 2006, pp. 4-11.

[6] Wang Q., Chen Q., Zhang D., Zeng M., Wu Y., and Gao Q. Shell-and-tube Heat Exchanger with Helical Baffles. United State Patent US 8,540,011 B2, 2013.

[7] T. W. Lodes and B. J. Field. The Challenge of Shell-and-Tube Heat Exchanger Mechanical Design. *Heat Transfer Engineering*, **8**(3), 1987, pp. 19-27.

[8] Panita B., Ojas D., Pranita D., Rhushabh G., and Tapobrata D. Study of Shell and Tube Heat Exchanger with the Effect of Types of Baffles. *Procedia Manufacturing*, **20**, 2018, pp. 195-200.

[9] Yonghua Y., Aiwu F., Suyi H., and Wei Liu. Numerical Modeling and Experimental Validation of Heat Transfer and Flow Resistance on the Shell Side of a Shell-and-tube Heat Exchanger with Flower Baffles. *International Journal of Heat and Mass Transfer*, **55**, 2012, pp.7561-7569.

[10] M.M. Elias, I.M. Shahrul, I.M. Mahbubul, R. Saidur, and N.A. Rahim. Effect of different Nanoparticle Shapes on Shell and Tube Heat Exchanger using different Baffle Angles and Operated with Nanofluid. *International Journal of Heat and Mass Transfer*, **70**, 2014, pp. 289-297.

[11] Jie Yang and Wei Liu. Numerical Investigation on a Novel Shell-and-tube Heat Exchanger with Plate Baffles and Experimental Validation. *Energy Conversion and Management*, **101**, 2015, pp. 689-696.

[12] Jian W., Huizhu Y., Simin W., Yulan X., and Xin T. Experimental Investigation on Performance Comparison for Shell-and-tube Heat Exchangers with different Baffles. *International Journal of Heat and Mass Transfer*, **84**, 2015, pp. 990-997.

[13] Xinting W., Nianben Z., Peng L., Zhichun L., Wei L. Numerical Investigation of Shell side Performance of a Double Shell side Rod Baffle Heat Exchanger. *International Journal of Heat and Mass Transfer*, **108**, 2017, 2029-2039.

[14] J. Lutcha and J. Nemcansky. Performance Improvement of Tubular Heat Exchanger by Helical Baffles. *Trans. Inst. Chem. Eng.*, **68**, 1990, pp. 263-270.

[15] Chen W., Jia-Gui Z. and Zhi-Fu S. Experimental Studies on Thermal Performance and Flow Resistance of Heat Exchangers with Helical Baffles. *Heat Transfer Engineering*, **30**(5), pp. 353-358.

[16] [16] Jian-Fei Z., Bin L., Wen-Jiang H., Yong-Gang L., Ya-Ling H., and Wen-Quan T. Experimental Performance Comparison of Shell-side Heat Transfer for Shell-and-tube Heat Exchangers with Middle-overlapped Helical Baffles and Segmental baffles. *Chemical Engineering Science*, **64**, 2009, pp. 1643-1653.

[17] Qiuwang W., Guidong C., Qiuyang C., and Min Z. Review of Improvements on Shell-and-Tube Heat Exchangers with Helical Baffles. Heat Transfer Engineering, **31**(10), 2010, pp. 836-853.

[18] Dogan E. Thermoeconomic Optimization of Baffle Spacing for Shell and Tube Heat Exchanger. *Energy Conversion and Management*, **47**(11-12), 2006, 1478-1489.

[19] Xinting W., Nianben Z., Zhichun L., and Wei L. Numerical Analysis and Optimization Study on Shell-side Performance of a Shell and Tube Heat Exchanger with Staggered Baffles. International Journal of Heat and Mass Transfer, **124**, 2018, pp. 247-259.

[20] Sadik K., Hongtan L., and Anchasa P. Heat Exchanger – Selection, Rating and Thermal Design, 3rd Edition, New York: CRC Press, 2012, pp. 387-395.